Available online at www.sciencedirect.com
SCIENCE DIRECT®
Superlattices and Microstructures 39 (2006) 340–347
Superlattices and Microstructures
www.elsevier.com/locate/superlattices

Catalyst effect on ZnO nanostructure shape

Caroline Andreazza-Vignolle[a,*], Pascal Andreazza[a], Dongxu Zhao[b]

[a] *Centre de Recherche sur la Matière Divisée, CNRS-Université d'Orléans, 1b rue de la Férollerie, 45071 Orléans Cedex 2, France*
[b] *Key Laboratory of Excited State Processes, Changchun Institute of Optics, Fine Mechanics and Physics, Chinese Academy of Sciences, 16 East Nan-Hu Road, Open Economic Zone, Changchun 130033, People's Republic of China*

Abstract

ZnO nanostructures are synthesized by a simple physical vapor phase transport technique using metallic clusters as the catalyst. Two kinds of catalyst are used: gold and platinum. The shape and growth direction were investigated by scanning electron microscopy, transmission electron microscopy and using X-ray diffraction. Depending on the metal used, we have shown that various kinds of nanostructures can be obtained. With gold catalyst, a homogeneous distribution of nanorods is observed. On the other hand, with platinum catalyst, two nanoribbon families are observed in addition to nanorods. A vapor–solid (VS) process with or without catalyst assistance is proposed to explain the nanoribbon growth and some photoluminescence measurements are presented.

1. Introduction

In recent years, the synthesis and characterization of one-dimensional (1D) semiconductor nanostructures have attracted much interest, because of their unique and fascinating optical, electrical, mechanical and thermoelectrical properties and potential technological applications. Nanodevices based on 1D semiconductors have been used in the realms of field-effect switches [1], single-electron transistors [2], biological and

---

[*] Corresponding author. Tel.: +33 2 38 25 53 78; fax: +33 2 38 25 53 76.
E-mail address: caroline.andreazza@univ-orleans.fr (C. Andreazza-Vignolle).

doi:10.1016/j.spmi.2005.08.060

chemical sensors [3] and light-emitting devices [4]. Among various nanostructured materials, ZnO is particularly important due to its wide band gap (3.37 eV) and large exciton binding energy (60 meV) [5]. One representative 1D ZnO nanostructure is the nanorod. Up to now, many methods have been used for preparing ZnO nanorods, including physical vapor deposition [6], vapor phase transport [7–9], chemical vapor deposition [10, 11], the surfactant assisted hydrothermal method [12,13], and the soft solution method [14]. The preparation of well-aligned high quality ZnO nanorod arrays with uniform length and controlled nucleation at low temperature is still desired, for well-aligned ZnO nanorod arrays can be used to fabricate ZnO nanorod Schottky diodes [15] and ZnO based nanorod heterojunctions [16–18]. ZnO exhibits a large and diverse range of growth morphologies such as nanocombs, nanorings, nanohelixes, nanobelts and nanowires which can lead to different applications [19–21].

In this paper, Au and Pt nanoclusters were used as catalysts to grow ZnO nanostructures. Gold is commonly used as a catalyst for ZnO growth in the literature [19]. However to our knowledge, this is the first time that Pt has been reported as a possible catalyst for ZnO nanostructure growth. In the following, the morphology and structure of ZnO nanostructures will be investigated and discussed. Moreover preliminary photoluminescence measurements will be presented.

2. Experimental

The ZnO nanorods were fabricated via a simple vapor phase transport process in a conventional furnace with a horizontal quartz tube. A mixture of commercial ZnO and graphite powders in a certain ratio (1:1) was placed in an alumina boat as the source material. Au and Pt nanoclusters were used as catalysts. These catalysts are obtained by a sputtering method in the case of gold and by an electron beam evaporation method in the platinum case. These metallic coatings are deposited on Si(100) wafers. They are composed of small metallic nanosized particles with an average diameter around 3 nm and 6 nm respectively for platinum and gold. Synthesis was carried out at 950 °C under a constant flow of Ar (99.99% purity) of 50 sccm for 30 min. After the reaction a light or dark gray layer was found on the substrate surface. Morphological and crystallographic properties of the as-grown samples were characterized by field emission scanning electron microscopy (FESEM—Hitachi S 4500), transmission electron microscopy (TEM—Philips CM20 operating at 200 kV) using a microscope equipped with an energy dispersive X-ray analyzer (EDX), selected-area electron diffraction (SAED) and X-ray diffraction (XRD—Philips X-pert diffractometer). In XRD measurements a symmetric configuration was used, in which the integral breadth of each diffracted intensity peak has been analyzed taking into account the instrumental (the geometrical element of the set-up) and spectral (CuKα_1 and Kα_2 X-ray linewidth) contributions in order to deduce the material intrinsic characteristics (microstrain and diffraction domain sizes). The photoluminescence (PL) measurements were carried out by using the 325 nm line of a He–Cd laser.

3. Results and discussion

The SEM image of ZnO nanorods directly grown on Au/Si substrate is shown in Fig. 1a. The nanorods grow randomly on the substrate surface. The size and shape distribution is

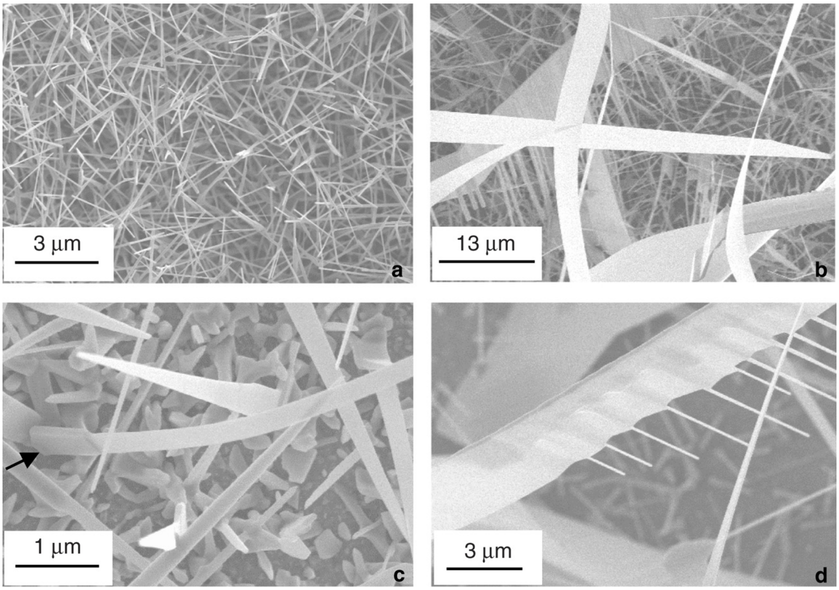

Fig. 1. SEM images of ZnO nanostructures, grown with Au (a) and Pt (b, c, d) catalysts.

homogeneous over the entire sample. The nanorod diameter is between 60 and 140 nm and the length is several microns, which increases with the time of deposition. The density of ZnO nanorods is $10/\mu m^2$. In the Pt case, the morphology looks different. Nanorods are present as in the Au case but some nanoribbons are also observed in the SEM image (Fig. 1b). The nanorod diameter is in the range of 30–70 nm; the length can reach 10 μm. In the case of nanoribbons, most of them have a uniform width along their entire length. The typical widths of nanoribbons vary over a large range of size: 200 nm to 7 μm and the thicknesses are 10–30 nm. Smaller ones grow from the surface substrate, as shown in the SEM image in Fig. 1c (indicated by an arrow). Bigger ones seem to grow above the nanorods and sometimes present some teeth growing perpendicularly to the nanoribbons leading to nanocomb structure. These teeth can be rods as shown in Fig. 1d or ribbons.

From TEM images and selected SAED patterns, the growth direction can be deduced. In the case of Au/Si substrates, nanorods are single crystalline and always grow along the [002] direction with a hexagonal shape according to the low index crystallographic face growth. These results have been widely described elsewhere [22]. As regards the Pt/Si substrates, the growth directions of nanorods are similar to those in the Au/Si case. However for nanoribbons, they differ. The TEM image in Fig. 2a shows a 4 μm width nanocomb. One face is straight; the other one is serrated which gives rise to the growth of teeth. Each tooth is parallel to every other one and has a length of several microns.

In this case each tooth is a rod (as shown on the SEM image in Fig. 2b) with a diameter of 100 nm. The SAED pattern shown in Fig. 2c indicates that this nanoribbon is single crystalline. The HRTEM filtered image of one tooth (nanorod) in Fig. 2d shows a lattice spacing of 0.26 nm indicating that the nanorod axis is the [002] axis of the ZnO

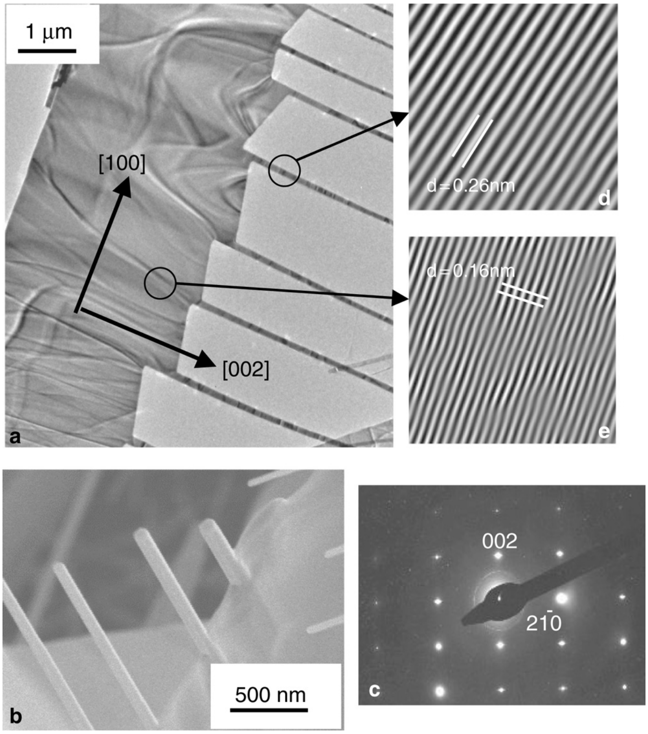

Fig. 2. (a) TEM image corresponding to ZnO nanoribbons presenting some teeth, (b) SEM image of nanoribbon teeth, (c) the SAED pattern corresponding to image (a) and HR filtered images of the nanoribbon (d) and the tooth (e).

wurtzite structure. Perpendicularly to this growth direction, the HRTEM filtered image of the nanoribbon in Fig. 2e shows a lattice spacing of 0.16 nm which confirms the preferred growth of ZnO nanoribbons along the [2$\bar{1}$0]* type direction in the reciprocal space, equivalent to the [100] type direction in the direct space.

Finally, at the tip of few nanoribbons, corresponding to the smaller ones, which grow from the surface substrate, a droplet appears (Fig. 3). This droplet has a diameter around 8 nm and the EDX analysis finding is consistent with a pure platinum composition. For the nanorods grown on Au/Si and Pt/Si substrates, no droplet was found on the tip at this growth temperature.

As shown in the diffraction spectrum of a sample grown with platinum as the catalyst (Fig. 4a), X-ray diffraction experiments reveal the presence of different deposited phases: zinc oxide, platinum fcc structure, in addition to the silicon substrate contribution ((004) reflection evidenced in a higher-*q* part of the spectra measurement, not presented in Fig. 4). Compared with that for a Pt catalyst ZnO sample, the XRD spectrum of the Au catalyst ZnO deposit (Fig. 4b) exhibits similar ZnO diffractive peaks and intensities with in addition a contribution from zinc metal phase. No preferential orientation is detected for ZnO nanostructures. Compared with the case for the gold catalyst sample or zinc oxide powders,

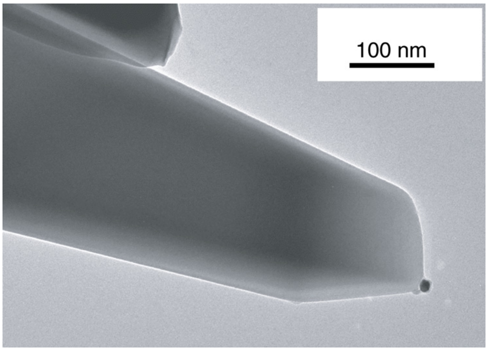

Fig. 3. A nanoribbon presenting a small Pt droplet on the tip.

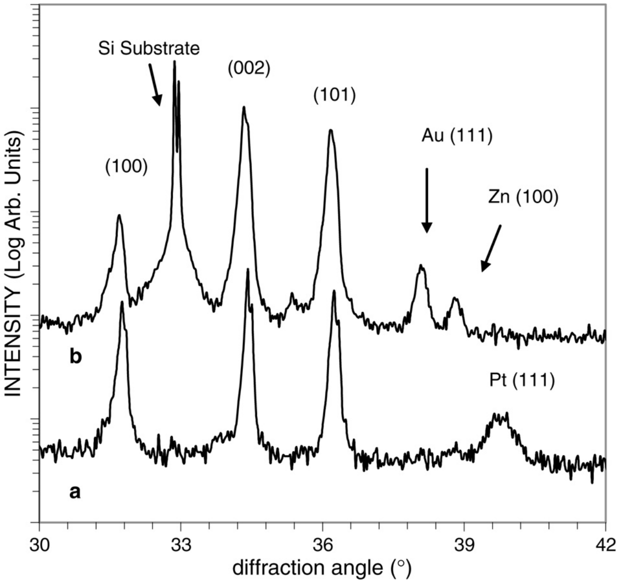

Fig. 4. XRD spectra of ZnO nanostructures grown with (a) Pt and (b) Au as the catalyst.

in the case of a Pt catalyst, ZnO diffractive peaks exhibit small shifts, which are due to lattice parameter expansion ($+3.5\times10^{-4}$ nm and $+2.6\times10^{-4}$ nm for a and c respectively), as shown in Fig. 5. In addition, the integral breadth (size and microdistortion contributions) can be compared for each X-ray line (Table 1), so the (002) broadening is very close to the intrinsic instrumental broadening of our diffraction set-up, which involves, in this direction, the domain size being macroscopic (above several μm) and the strains being negligible. This is not the case in the perpendicular [100]* type reciprocal space directions (corresponding to the (100) peak) which exhibit a higher value similar to that obtained with

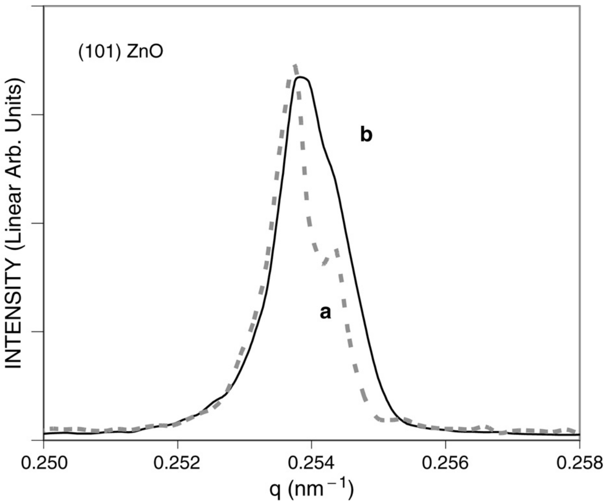

Fig. 5. Zoom of the XRD spectra on the (101) diffraction peak: (a) Pt and (b) Au as the catalyst.

Table 1
XRD data (2θ position and integral breadth) of ZnO contributions for Au catalyst and Pt catalyst samples

Peak	Au catalyst		Pt catalyst	
	2θ position (°)	Int. breadth (°)	2θ position (°)	Int. breadth (°)
(100)	31.783	0.100	31.745	0.116
(002)	34.430	0.115	34.412	0.072
(101)	36.263	0.122	36.237	0.100

Au catalyst ZnO nanorods. These results indicate that ZnO nanostructures obtained with Pt catalyst present a higher crystalline quality close to that of a perfect crystal.

The growth of nanostructures is strongly dependent on the partial pressures of the reactants (Zn and O_2), on the configuration of the experimental set-up (growth temperature, gas flow) and the starting material. In our case, except the nature and size of the catalyst, all other parameters are similar.

The present study revealed that the nature and size of the catalyst had a significant effect on the morphology of the final nanostructures. Firstly the catalyst is present at the surface substrate in the form of nanoparticles. The initial sizes are 3 nm and 6 nm respectively for platinum and gold. Even if there is a reorganization of the catalyst with increasing temperature, the final catalyst size at the beginning of the ZnO growth is inferior in the case of platinum, leading to the growth of smaller nanorods. In both cases, the nanorod growth follows a catalyst assisted vapor–solid process consistent with the fact that no droplet appears on the nanorod tip [23].

Secondly the use of various catalysts leads probably to different reactivity between zinc and oxygen vapor and catalyst nanoparticles. Moreover the solubility and the ability to

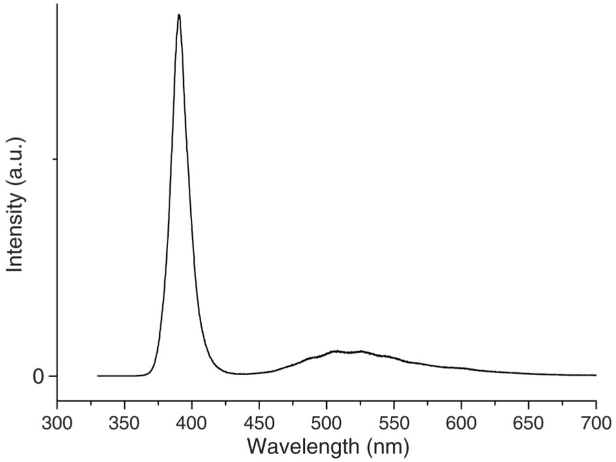

Fig. 6. PL spectrum of ZnO nanorods grown with Au as the catalyst.

react with oxygen may well be dependent and consequently differ from one catalyst to another. These considerations could explain the different morphologies observed in our samples at the substrate surface: nanorods only in the gold case and nanorods–nanoribbons in the platinum case. This change of morphology has already been correlated with a variation of partial pressures in the literature but mainly experimentally explained by a modification of gas flow rate [20] or change of starting materials [21]. Afterwards, a second growth takes place above the first one. The nucleation of these large nanoribbons may follow a growth process without the use of catalyst as already observed in the literature, leading to the formation of nanobelts [24]. These two different morphologies lead to various preferential growth directions: [001] for nanorods and [100] for nanoribbons. These two directions correspond to fast growth directions. The morphology of nanoribbons is dominated by the non-polar surfaces of the wurtzite ZnO structure (($2\bar{1}0$) and (010)) which have lower energies than the (001) one.

Finally, as mentioned above, some nanoribbons present a Pt droplet at the top. We could probably attribute this phenomenon (occasionally observed) to the fact that in the case of platinum, the size distribution of the catalyst nanoparticles could be large. In consequence, some catalyst droplets could be small enough to be in liquid phase at 950 °C leading to a Vapor–Liquid–Solid (VLS) growth and consequently to the appearance of a small Pt droplet. In this process Zn vapor could be dissolved into Pt nanoclusters on the Si substrate surface at this temperature by forming a liquid alloy. Then with further oxidation ZnO nanostructures grow.

Fig. 6 shows the PL spectra of ZnO nanorods grown with a gold catalyst. A strong ultraviolet emission could be observed in the spectrum, which could be attributed to near band gap exciton related emission. Moreover a weak emission band in the visible region is also present in the spectrum. This emission is thought to have originated from a deep level defect in ZnO. Some PL measurements on nanostructures grown with the Pt catalyst need to be done soon.

4. Conclusions

In summary, various shaped ZnO nanostructures could be synthesized on Si substrate by using different metal catalysts. In the case of gold, nanorods are obtained with [001] preferential growth direction. With platinum, some nanoribbons, with preferential [100] growth direction, are also observed. Two nanoribbon families are evidenced. The first one nucleates directly on platinum particles at the substrate surface according to a catalyst assisted VS growth. For the second one, the nucleation takes place above the primary growth, leading sometimes to hierarchical nanostructures as nanoribbons with teeth. This nucleation follows a VS growth without catalyst assistance.

References

[1] G.T. Kim, J. Muster, V. Krstic, J.G. Park, Y.W. Park, S. Roth, M. Burghard, Appl. Phys. Lett. 76 (2000) 1875.
[2] N.J. Stone, H. Ahmed, Appl. Phys. Lett. 73 (1998) 2134.
[3] Y. Cui, Q. Wei, H. Park, C.M. Lieber, Science 293 (2001) 1289.
[4] M.H. Huang, S. Mao, H. Feick, H. Yan, Y. Wu, H. Kind, E. Weber, R. Russo, P. Yang, Science 292 (2001) 1897.
[5] H. Chik, J. Liang, S.G. Cloutier, N. Kouklin, J.M. Xu, Appl. Phys. Lett. 84 (2004) 3376.
[6] Y.C. Kong, D.P. Yu, B. Zhang, W. Fang, S.Q. Feng, Appl. Phys. Lett. 78 (2001) 407.
[7] M.H. Huang, Y. Wu, H. Feick, N. Tran, E. Weber, P. Yang, Adv. Mater. 13 (2001) 113.
[8] Y.W. Wang, L.D. Zhang, G.Z. Wang, X.S. Peng, Z.Q. Chu, C.H. Liang, J. Cryst. Growth 234 (2002) 171.
[9] H.Z. Zhang, X.C. Sun, R.M. Wang, D.P. Yu, J. Cryst. Growth 269 (2004) 464.
[10] J.J. Wu, S.C. Liu, J. Phys. Chem. B 106 (2002) 9546.
[11] J.J. Wu, S.C. Liu, Adv. Mater. 14 (2002) 215.
[12] X.M. Sun, X. Chen, Z.X. Deng, Y.D. Li, Mat. Chem. Phys. 78 (2002) 99.
[13] L. Vayssieres, Adv. Mater. 15 (2003) 464.
[14] C.H. Hung, W.F. Whang, Mat. Chem. Phys. 82 (2003) 705.
[15] W.I. Park, G.C. Yi, J.-W. Kim, S.-M. Park, Appl. Phys. Lett. 82 (2003) 4358.
[16] W.I. Park, G.-C. Yi, M. Kim, S.J. Pennycook, Adv. Mater. 15 (2003) 526.
[17] W.I. Park, G.C. Yi, Adv. Mater. 16 (2004) 87.
[18] S.W. Jung, W.I. Park, G.C. Yi, M. Kim, Adv. Mater. 15 (2003) 1358.
[19] Z.L. Wang, J. Phys.: Condens. Matter 16 (2004) R829.
[20] Z. Chen, N. Wu, Z. Shan, M. Zhao, S. Li, C.B. Jiang, M.K. Chyu, S.X. Mao, Scr. Mater. 52 (2005) 63.
[21] Y.H. Leung, A.B. Djurisic, J. Gao, M.H. Xie, W.K. Chan, Chem. Phys. Lett. 385 (2004) 155.
[22] D.X. Zhao, C. Andreazza, P. Andreazza, J. Ma, Y. Liu, D.Z. Shen, Chem. Phys. Lett. 408 (2005) 335.
[23] D.X. Zhao, C. Andreazza, P. Andreazza, J.G. Ma, Y.C. Liu, D.Z. Shen, Chem. Phys. Lett. 399 (2004) 522.
[24] Z.W. Pan, Z.R. Dai, Z.L. Wang, Science 291 (2001) 1947.